

An unsupervised approach towards promptable defect segmentation in laser-based additive manufacturing by Segment Anything

Israt Zarin Era¹, Imtiaz Ahmed^{1*}, Zhichao Liu^{1*}, Srinjoy Das^{1,2*}

¹Industrial and Management Systems Engineering, West Virginia University, Morgantown, 26505, WV, USA.

²School of Mathematical and Data Sciences, West Virginia University, Morgantown, 26505, WV, USA.

*Corresponding author(s). E-mail(s): imtiaz.ahmed@mail.wvu.edu; zhichao.liu@mail.wvu.edu; srinjoy.das@mail.wvu.edu; Contributing authors: ie0005@mix.wvu.edu;

Keywords: Laser-Based Additive Manufacturing, Segment Anything, Defect Segmentation, Visual Prompts Tuning, Anomaly Detection.

Foundation models are currently driving a paradigm shift in computer vision tasks for various fields including biology, astronomy, and robotics among others, leveraging user-generated prompts to enhance their performance. In the manufacturing domain, accurate image-based defect segmentation is imperative to ensure product quality and facilitate real-time process control. However, such tasks are often characterized by multiple challenges including the absence of labels and the requirement for low latency inference among others. To address these issues, we construct a framework for image segmentation using a state-of-the-art Vision Transformer (ViT) based Foundation model (Segment Anything Model) with a novel multi-point prompt generation scheme using unsupervised clustering. We apply our framework to perform real-time porosity segmentation in a case study of laser base powder bed fusion (L-PBF) and obtain high Dice Similarity Coefficients (DSC) without the necessity for any supervised fine-tuning in the model. Using such lightweight foundation model

inference in conjunction with unsupervised prompt generation, we envision the construction of a real-time anomaly detection pipeline that has the potential to revolutionize the current laser-based additive manufacturing processes, thereby facilitating the shift towards Industry 4.0 and promoting defect-free production along with operational efficiency.

Real-time vision-based quality inspection [1] and control are essential for ensuring the reliability of the final product, particularly in industries such as aerospace and automotive where precision is non-negotiable for safety. Defect segmentation plays a crucial role in this process, as it aids in the root cause analysis of anomalies by precisely identifying and locating deviations from the expected standards. With the advent of Industry 4.0, [2], defect segmentation has become integral to both preventive maintenance and corrective actions within the production pipeline to improve process efficiency and ensure high-quality products. However, it is challenging to carry out such tasks in industrial settings compared to medical or natural instances. Unlike medical or biological imaging domains where the data structure is relatively standardized [3–5] and labels are often available, industrial defects have diverse forms, low signal-to-noise ratios, and often insufficient labeling. This complexity necessitates the development of more adaptable and versatile segmentation techniques. Consequently, there is a critical need for approaches that are more customized and specifically tailored to industrial defect segmentation [6, 7]. In this paper, our discussion centers on a case study from [8], focusing on image segmentation for defects observed in cylindrical parts printed through the L-PBF process. Despite its wide adoption in various industries, L-PBF is susceptible to defects, such as porosity, cracking, and geometric distortions. Porosity is a very common defect in L-PBF due to lack of fusion, entrapped gas, and keyholes [8, 9]. Porosity directly affects mechanical properties like tensile strength, stiffness, and hardness thereby compromising the quality of the final product. [10]. Non-destructive tests like high-resolution X-ray Computed Tomography (XCT) are widely used to isolate and locate pores in the fabricated parts [8–10]. However, identifying and measuring inter-layer porosity from XCT data can be tenuous and challenging and to address this, machine learning-driven image segmentation has been adopted for such tasks which has significantly improved the overall process as well as product quality.

Semantic segmentation [11] is a computer vision task that assigns a label to every pixel and helps to understand a pixel-wise mapping of the contents in an image. In the rapidly advancing field of Artificial Intelligence (AI), the domain of image segmentation within manufacturing is undergoing significant transformation. Traditional machine learning techniques like Support Vector Machine [12] and Random Forest [12, 13], often combined with methods like Bernsen Thresholding [14] and Otsu Thresholding [15], are increasingly being superseded by deep learning-based algorithms. A notable example is the use of U-Net for defect segmentation in Laser-based Additive Manufacturing (LBAM). Originally designed for medical image segmentation, U-Net [16], has emerged as a leading tool for segmentation in surface anomalies [17], 3D volumetric defects [18], and 3D geometry reconstruction [19], and established itself as the benchmark in semantic segmentation of the LBAM defects by achieving remarkable accuracy. However, in real-world scenarios, most of the LBAM data are either

non-labeled or limited in sample size. This directly conflicts with the conventional supervised training approach of U-Net and its variants. Transfer learning [20], even when utilizing pre-trained U-Net models, still necessitates the partial training of the decoder using labeled data [21]. In addition, pre-trained models, may not fully align with the target data during domain shift and that can greatly increase the complexity of fine-tuning. This challenge can be resolved by using Foundation models [22], such as the Segment Anything Model (SAM) [23] shown in Fig. 4. Developed by Meta, SAM is recognized for initiating a major shift in the field of image segmentation. This model can utilize prompts [24, 25] to carry out specific segmentation tasks without prior training. However, a limitation arises as most visual prompts, i.e., bounding boxes and points, typically depend on human-generated annotations or interventions [26], which may not always be feasible to provide. To overcome this, in this paper, we introduce a simple yet novel framework for segmenting porosity in XCT images of parts produced by L-PBF. This framework applies SAM in conjunction with an unsupervised method for generating contextual prompts. Our framework significantly enhances the process of image segmentation in manufacturing settings by introducing an automated strategy for generating prompts directly from the data. This approach is particularly suited for real-world manufacturing tasks. It facilitates efficient prompting for the Segment Anything Model (SAM), enabling it to perform semantic segmentation and predict masks with higher accuracy.

Starting with their remarkable success in natural language processing (NLP) [27], foundation models are now being widely adopted for computer vision tasks [28, 29]. These are machine learning models that are trained using self-supervised learning techniques on vast amounts of unlabeled data to perform inference on target data with little or no fine-tuning. They are versatile and can be applied to a broad range of tasks without requiring specific training for individual applications. This makes them very versatile and useful for a wide range of applications [22]. Most foundation models in computer vision are built on Vision Transformer Encoder and Decoder architecture (ViTs) [30, 31]. Now, compared to traditional Convolutional Neural Networks (CNNs) based deep learning models [32] which have been extensively used for various tasks in computer vision, ViTs exhibit distinct characteristics. CNNs are adept at inference tasks such as image recognition and segmentation by generating feature maps that emphasize local image details and exhibit shift invariance [33]. However, their performance may suffer during significant changes in the orientation of objects or patterns in the image. ViTs, on the other hand, rely on an attention mechanism, enabling them to capture global context and long-range dependencies in addition to local information [34]. Multi-headed Attention in ViTs further enhances their capability by allowing different heads to focus on various aspects of the input, thereby producing a comprehensive representation combining both local and global contexts [31]. These models outperform CNNs in tasks like image classification, object detection, and semantic segmentation by simultaneously considering information from various parts of the input image [35]. The ViT-based architecture of SAM has three key components: an image encoder as the initial processing step, a prompt encoder that accepts both sparse prompts (bounding boxes, points, texts) and dense prompts (masks), and a lightweight mask decoder that generates masks using image embedding, prompt embedding, and

an output token in Fig. A1. However, in spite of several initial reported successes, foundation models such as SAM have been found to face challenges in real-world computer vision tasks, with ViTs showing lower generalization performance and as well as reduced accuracy under significant domain shifts [35]. For example, despite its huge success in biological image segmentation, SAM failed to segment concealed objects in camouflaged animals, industrial defects, and medical lesions [6]. Similarly, for the case of our application, we find that directly applying SAM to the XCT images of the defects does not produce optimal results and therefore we opted to address this problem with the help of visual prompting [24, 36]. Our research reveals that integrating contextual prompt generation into the SAM framework, to provide weak supervision [37], significantly enhances the model’s performance, resulting in a marked improvement in the quality of the final segmentation.

We studied the XCT grayscale surface images of different layers of two CoCr alloy 3D cylindrical specimens A and B with 10.19% and 2.09% porosity (Fig. A4) respectively fabricated by the L-PBF process [8]. As is often the case with real-world manufacturing data sets, there are no pre-existing labels available for this data. Our approach focuses on conducting the defect segmentation of these unlabeled images using SAM along with prompts generated by unsupervised clustering. The proposed framework consists of three main steps: data preprocessing, prompt generation, and SAM-based inference to predict the final masks in Fig. 1. For our study, we explore the point prompt option available in SAM and use the location coordinates of the pores that make up the foreground. In the data preprocessing step we first select a set of images from specimen A (Fig. A4), run unsupervised K-means clustering to group them in respective clusters and obtain the centroid images. In the context of our dataset, we employ Binary Thresholding [38] to partition each centroid image into foreground representing defects, and background encompassing the remaining data. Then we randomly select a small subset of 2D location coordinates from the foreground pixels of these stored centroid images and their corresponding labels and use them as prompts for SAM during inference. Generating prompts using centroids of clustered images avoids the overhead of creating prompts from selected regions of each image. In our experiments, we observe that using such centroid-based prompts does not impact the segmentation accuracy as compared to using prompts from each image. We first run SAM inference on the same set of images used for clustering to generate the centroid-based prompts (image set 1). Following this, we select another random subset of images from the same specimen A which was not used for clustering, and then perform SAM-based inference on this dataset (image set 2). We apply the same methodology to the XCT images of Specimen B, the results are discussed in the Appendix. Our primary goal is to maintain an unsupervised methodology throughout, both in generating prompts from the data and in executing real-time defect segmentation for images.

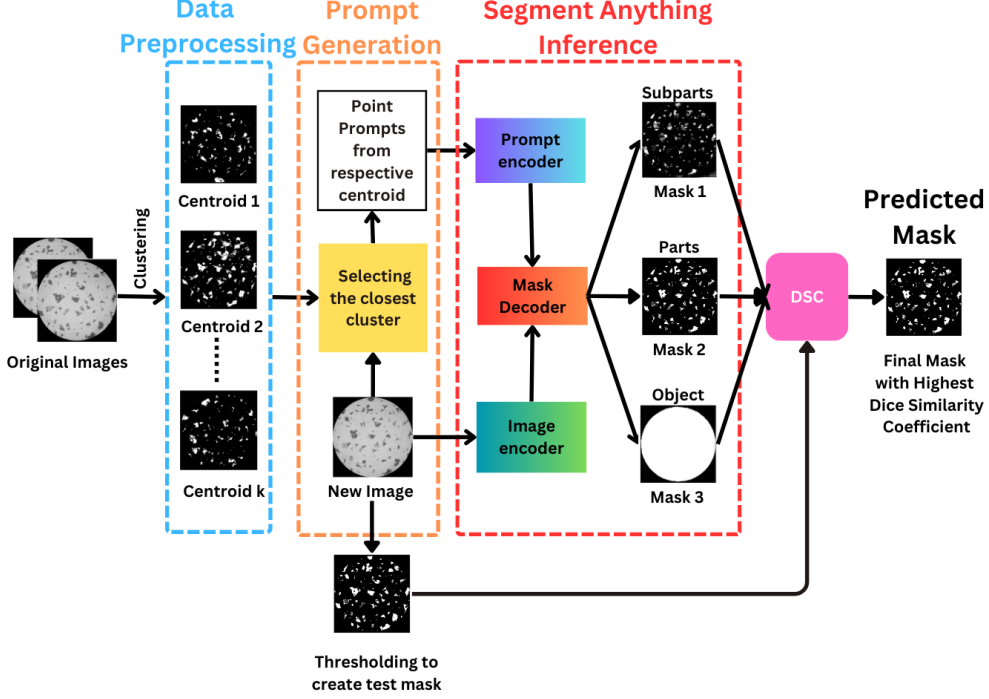


Fig. 1 The framework of unsupervised prompt generation with Segment Anything Model.

SAM is originally trained to generate a valid segmentation mask for any given input and prompts. It implies that, even when a prompt is ambiguous and can pertain to multiple objects, the output is expected to be a reasonable mask for one of those objects. SAM can return multiple masks of one image if enabled and the masks usually are either sub-parts, parts, or the whole object with different segmentation accuracy (Fig. 1). We select the mask returning the parts each time because the ones returning the entire circular surface of the cylindrical specimen are not suitable for our application and the one returning sub-parts of the defects provide only partial information about the defects. To evaluate the performance of our framework, it is required to have labels that distinguish defects from the remaining components in the images. However, as discussed earlier, our real-world manufacturing data set lacks labels, and generating ground truth masks manually for such a large data set is not a viable option. Hence, we apply K-means thresholding [21] with median filtering [39] and binary thresholding to create binary masks to generate comparisons with the masks generated by SAM. The final masks generated by SAM utilizing our framework, along with their centroids for distinct clusters and the thresholded binary masks are presented in Fig. 3. We calculate the Dice Similarity Score (DSC)[40] to measure the accuracy of segmentation.

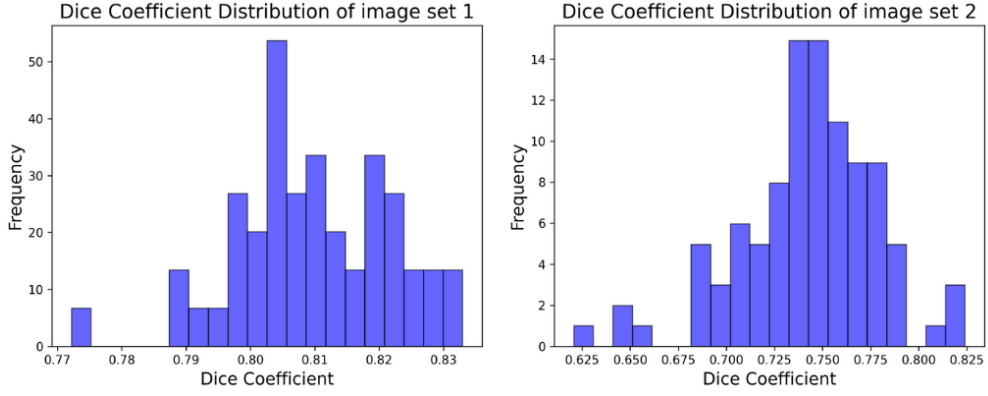


Fig. 2 The distribution of DSC values from image set 1 (left) and image set 2 (right) from specimen A. DSC values from image set 2 are slightly lower compared to that of image set 1 because we do not update the centroids for image set 2.

Without any prompt, SAM returns ambiguous masks of the defects with very low DSC values in the range of 0.07 to 0.48. It is therefore evident that in the absence of specific guidance, SAM faces challenges in accurately recognizing the intricate details of defects and understanding the variability within the data. On the other hand, employing the centroid-based prompt generation method described earlier, in conjunction with the image set 1 from specimen A, yields Dice Similarity Coefficient (DSC) values with an average of 0.81, a maximum of 0.83, and a minimum of 0.77. Subsequently, we employ a similar approach on image set 2 from specimen A, resulting in DSC values averaging 0.75, with a maximum of 0.82 and a minimum of 0.62. The distribution graphs illustrating Dice Similarity Coefficient (DSC) values obtained from these two image sets are shown in Fig. 2.

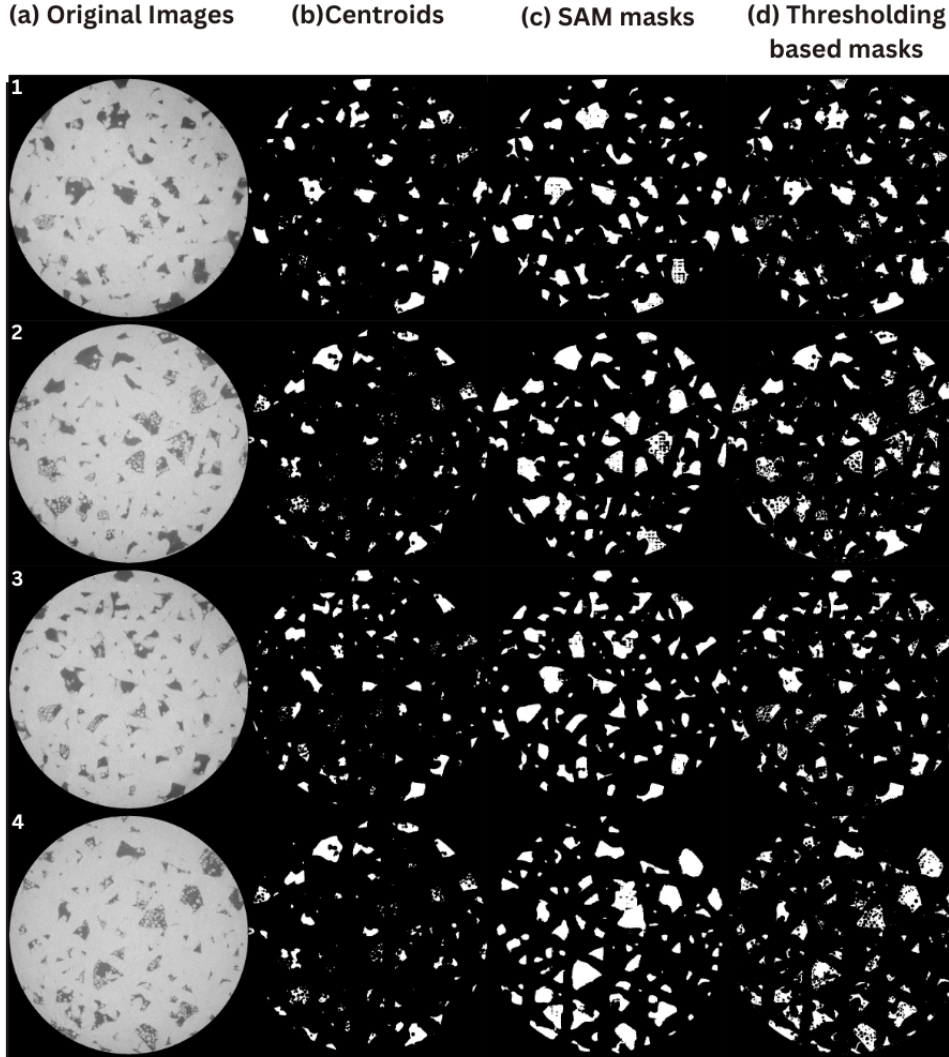


Fig. 3 Predictions by SAM using our prompts. Rows 1,2,3 represent examples from image set 1. Row 4 represents an example from image set 2. (a.1) Image belonging to cluster 1, (b.1) Centroid image of cluster 1 after thresholding, (c.1) Predicted mask by SAM, (d.1) Corresponding ground truth mask, (a.2) Image belonging to cluster 2, (b.2) Centroid image of cluster 2 after thresholding, (c.2) Predicted mask by SAM, (d.2) Corresponding ground truth mask, (a.3) Image belonging to cluster 3, (b.3) Centroid image of cluster 3 after thresholding, (c.3) Predicted mask by SAM, (d.3) Corresponding ground truth mask, (a.4) Image from set 2, (b.4) The closest centroid, (c.1) Predicted mask by SAM, (d.1) Corresponding ground truth mask

From our experiments we observe that SAM with our unsupervised prompt generation framework, demonstrates proficiency in detecting and isolating defects within

images of the industrial specimens, making it suitable for real-time anomaly detection. Through segmentation, anomaly detection can be accomplished by identifying the presence of defects in the samples [41, 42] or by applying a threshold limit to quantify the number of defects. It can be set by the user according to desired mechanical properties like tensile tests for the final products of a specific material [43, 44]. Therefore, the prospect of a real-time anomaly detection pipeline driven by foundation models like SAM holds the promise of significant advancement over current methodologies in the domain of LBAM. SAM's lightweight mask decoder [23] has shown significant potential to deal with machine latency issues and control requirements. For a single RGB image of size 1010 pixels by 984 pixels using multiple point prompts, the total run time to generate three valid masks ranges from 3.8 to 4.4 seconds. Moreover, integrating Internet of Things (IoT) sensors [45] in the system can enhance operational efficiency with uninterrupted communication between devices e.g. cameras, deployment interfaces, and production systems. Our centroid-based prompt generation methodology for performing segmentation with SAM enables a simple and seamless framework that can function without human interaction. Our procedure facilitates the construction of a real-time anomaly detection pipeline as shown in Fig. 4 thereby enabling online process control using foundation model-based inference to ensure uninterrupted production and achieve defect-less products.

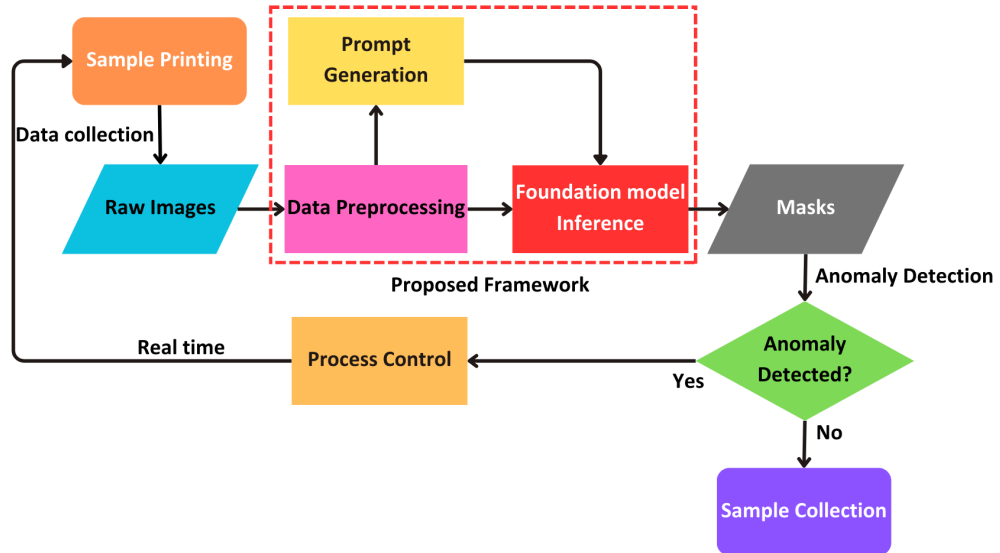


Fig. 4 Anomaly Detection Pipeline with Foundation Model Inference, enabling Industry 4.0 Integration

SAM has limitations when it comes to identifying concealed and intricate defect patterns without a certain level of supervision. However, our novel unsupervised approach to generating point prompts for guiding SAM holds great promise as it can potentially eliminate the need for preexisting labels and help address real-time production machine latency issues. Even when applied to out-of-distribution data from another specimen (specimen B) as depicted in Fig. A5, it exhibited robust performance. While SAM attains high accuracy in defect segmentation through our unsupervised prompt generation approach, a performance plateau is still evident in the performance curve in Fig. A2. To further enhance accuracy, there is a clear and urgent need for a specialized foundation model designed to recognize the complex features inherent in industrial defects within the manufacturing domain. Our ongoing work focuses on designing such specialized model which represents a significant step in harnessing their full potential to address the evolving and distinctive challenges of manufacturing industries.

Appendix A

Architecture of Segment Anything Model The architecture of SAM consists of an image encoder, a prompt encoder, and a mask decoder. The input image is first divided into fixed-size non-overlapping patches. These patch embeddings along with positional embeddings which represent the spatial information of different elements in the input sequence are used as inputs to the image encoder. The image encoder which employs a Masked Autoencoder (MAE) [46] pre-trained Vision Transformer (ViT) takes these embeddings and generates output tokens that capture the global context from the input. The prompt encoder accommodates two types of prompts: sparse prompts (bounding boxes, points) represented through positional embeddings combined with image embeddings, and dense prompts (masks) embedded via convolution and element-wise summation using the image embeddings. The mask decoder, based on a modified transformer decoder block [31], facilitates bidirectional self-attention and cross-attention and processes the image embeddings along with the prompt and output tokens. In the final stage a Multi-Layer Perceptron (MLP) in conjunction with a linear classifier is used to compute the mask foreground probability at each image location.

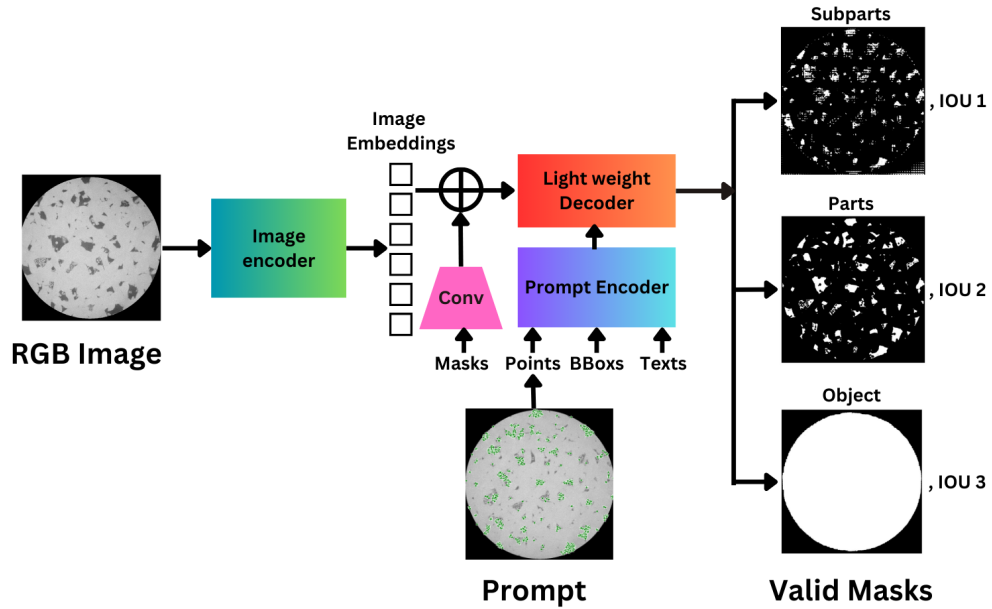


Fig. A1 SAM architecture redrawn from [8]

Visual Prompts generation approach Visual prompts were first conceptualized in [47] using analogous ideas from Natural Language Processing (NLP). This technique addresses the challenge of adapting a pre-trained source model to a specific task without necessitating any target-specific modifications like fine-tuning a pre-trained

model [24, 36]. For our experiments, we employ unsupervised k-means clustering to create centroid images from each cluster and then divide them into foreground and background pixels using binary thresholding. Following this we randomly sample a subset of the location coordinates of the foreground pixels from the respective centroid images and use them as prompts to create segmentation masks for both specimens A and B.

We evaluated the model’s performance by varying the percentage of location coordinates extracted from the foregrounds of each centroid image to be used as point prompts. Our findings indicate a positive correlation between the total number of point prompts and the performance of SAM, as depicted in Fig. A2. A comparison of predicted masks for different numbers of prompts generated from centroid image foreground is illustrated in Fig. A3. The experimentation encompassed subsets ranging from 0.1% to 18% of the total point prompts. Our experiments were restricted to using 18% of the total prompts owing to memory constraints beyond this limit.

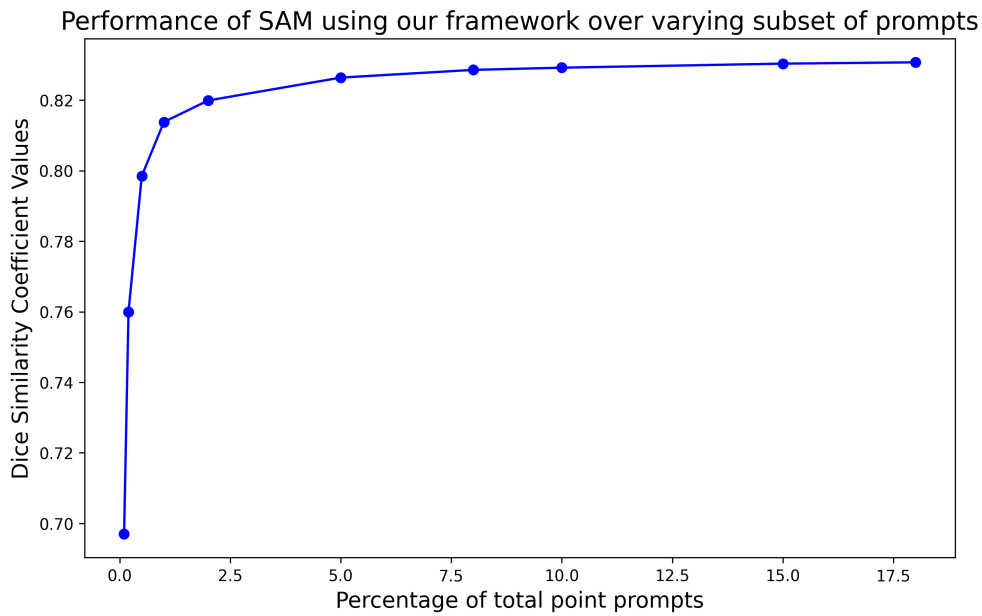


Fig. A2 Prediction performance of SAM versus percentage of total point prompts using our framework

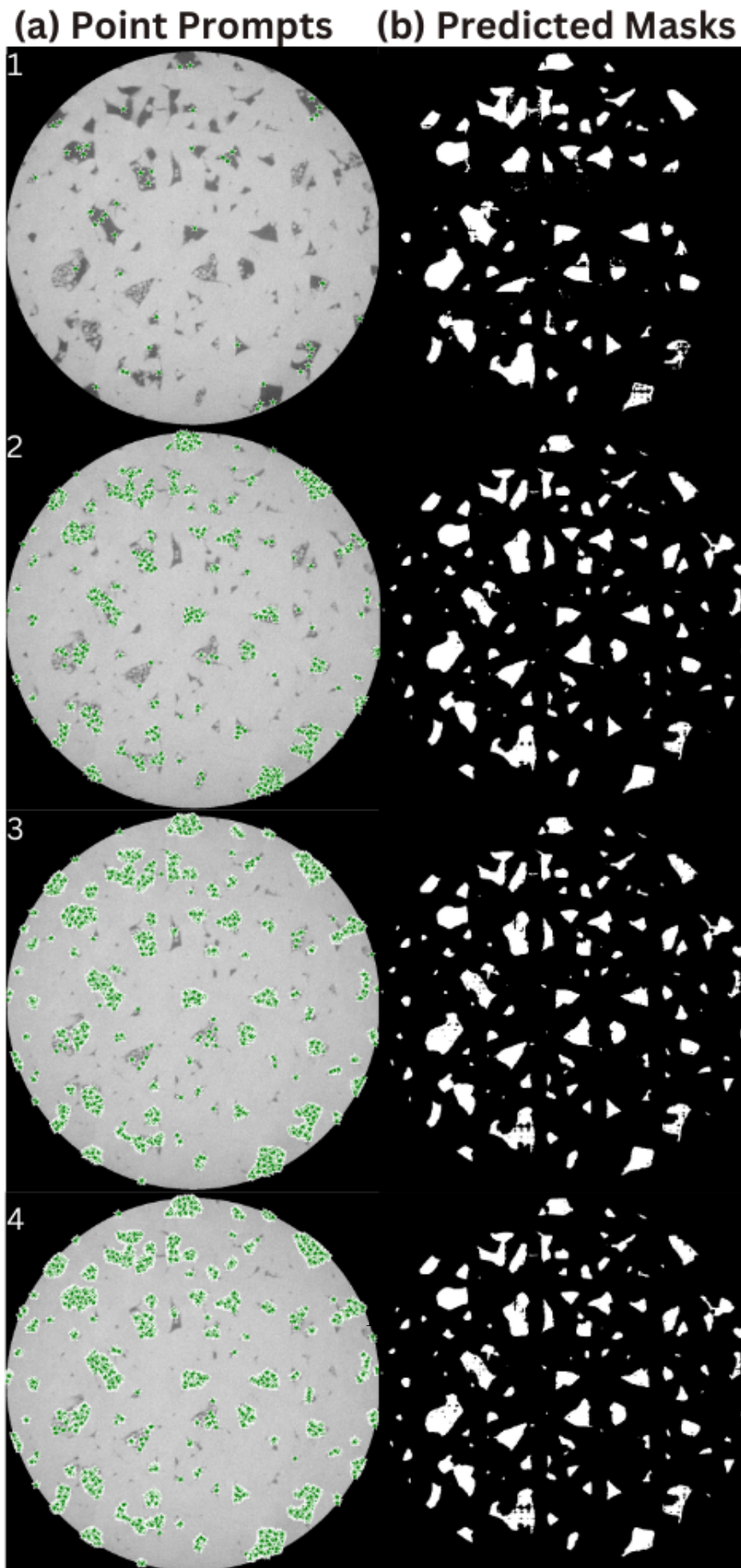


Fig. A3 Visual comparison of SAM performance with increasing number of prompts extracted from centroid image foregrounds: (a.1) 0.1% of total possible point prompts and (b.1) the corresponding predicted masks with DSC value of 0.697; (a.2) 2% of total possible point prompts and (b.2) the corresponding predicted masks with DSC value of 0.813; (a.3) 10% of total possible point prompts and (b.3) the corresponding predicted masks with DSC value of 0.828; (a.4) 18% of total possible point prompts and (b.4) the corresponding predicted masks with DSC value of 0.829

Dataset The data presented in this study is derived from [8], where Cobalt-chrome alloy specimens, containing elements such as Co, Cr, Mo, Si, Mn, Fe, C, and Ni, were fabricated through laser-based powder bed fusion (PBF) processes. The study involved high-resolution X-ray computed tomography (XCT) scans on the L-PBF manufactured CoCr specimens to explore the effects of varying processing parameters, specifically scan speed and hatch spacing on pore structure formation and overall porosity. For our investigation, we used the data from two specimens, one with fewer but larger individual pores (10.19%) with more pronounced laser tracks and another with minimum pores (2.09%). This dataset provides a compelling example of real-life defects encountered in additive manufactured parts.

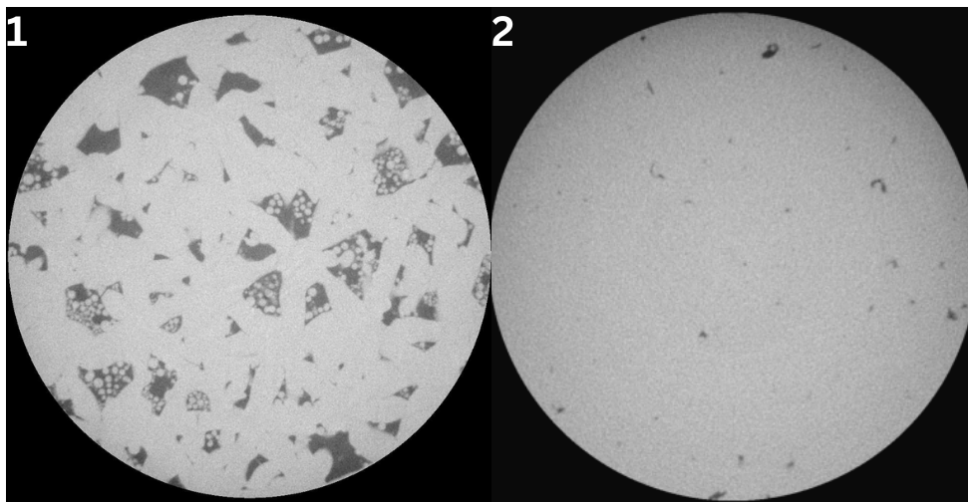


Fig. A4 XCT images showing the surface topology of defects of two CoCr alloy cylindrical discs; (1) Specimen A with 10.19% porosity and (2) Specimen B with 2.09% porosity [8].

Out-of-distribution results To test the robustness of this framework, we conducted testing using out-of-distribution images derived from a 3D printed cylindrical part labeled as specimen B in Fig. A4. It is remarkable to note that when applying point prompts generated from the centroids of specimen A (as depicted in Fig. A4), we still obtained masks of high quality using our framework with SAM for this entirely different cylindrical 3D specimen B as shown in Fig. A5. This result underscores the adaptability and effectiveness of our approach across diverse datasets and highlights its potential for broader applicability in quality assessment for 3D printed parts.

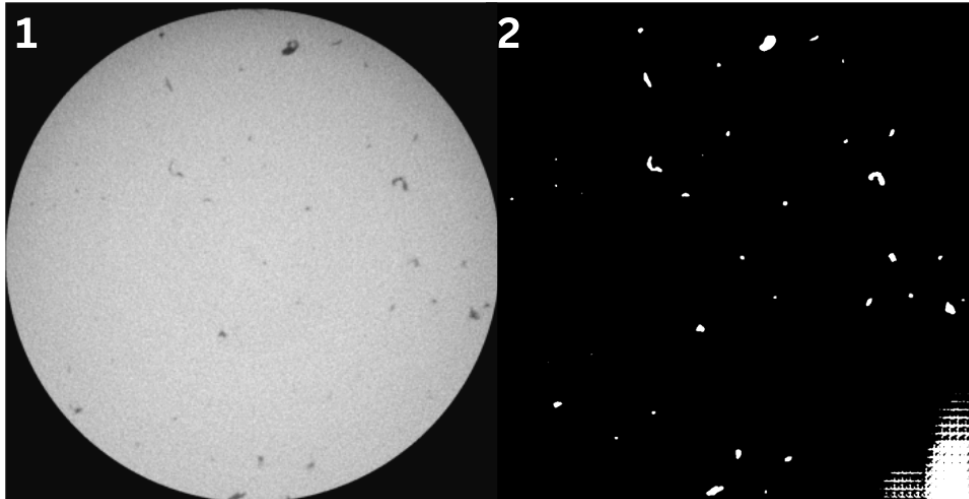


Fig. A5 Prediction by SAM using prompts on specimen B with 2.09% porosity[8].

Declarations

- **Funding:** This material is based upon work supported by the National Science Foundation under Grant No. 2119654. Any opinions, findings, conclusions, or recommendations expressed in this material are those of the author(s) and do not necessarily reflect the views of the National Science Foundation.
- **Conflict of interest/Competing interests:** As authors of this work, we declare that we have no conflicts of interest.
- **Availability of data and materials:** The dataset used and analyzed during the current study are available in NIST Engineering Laboratory's repository, <https://www.nist.gov/el/intelligent-systems-division-73500/cocr-am-xct-data>
- **Code availability:** The underlying code for this study is not publicly available but may be made available on reasonable request from the corresponding author.
- **Acknowledgments:** The authors would like to acknowledge the Pacific Research Platform, NSF Project ACI-1541349, and Larry Smarr (PI, Calit2 at UCSD) for providing the computing infrastructure used in this project.

References

- [1] Gao, Y., Li, X., Wang, X.V., Wang, L., Gao, L.: A review on recent advances in vision-based defect recognition towards industrial intelligence. *Journal of Manufacturing Systems* **62**, 753–766 (2022)
- [2] Oztemel, E., Gursev, S.: Literature review of industry 4.0 and related technologies. *Journal of intelligent manufacturing* **31**, 127–182 (2020)

- [3] Azad, B., Azad, R., Eskandari, S., Bozorgpour, A., Kazerouni, A., Rezik, I., Merhof, D.: Foundational models in medical imaging: A comprehensive survey and future vision. arXiv preprint arXiv:2310.18689 (2023)
- [4] Mazurowski, M.A., Dong, H., Gu, H., Yang, J., Konz, N., Zhang, Y.: Segment anything model for medical image analysis: an experimental study. *Medical Image Analysis* **89**, 102918 (2023)
- [5] Wu, J., Fu, R., Fang, H., Liu, Y., Wang, Z., Xu, Y., Jin, Y., Arbel, T.: Medical sam adapter: Adapting segment anything model for medical image segmentation. arXiv preprint arXiv:2304.12620 (2023)
- [6] Ji, G.-P., Fan, D.-P., Xu, P., Cheng, M.-M., Zhou, B., Van Gool, L.: Sam struggles in concealed scenes—empirical study on” segment anything”. arXiv preprint arXiv:2304.06022 (2023)
- [7] Moenck, K., Wendt, A., Prünke, P., Koch, J., Sahrhage, A., Gierecker, J., Schmedemann, O., Kähler, F., Holst, D., Gomse, M., et al.: Industrial segment anything—a case study in aircraft manufacturing, intralogistics, maintenance, repair, and overhaul. arXiv preprint arXiv:2307.12674 (2023)
- [8] Kim, F., Moylan, S., Garboczi, E., Slotwinski, J.: Investigation of pore structure in cobalt chrome additively manufactured parts using x-ray computed tomography and three-dimensional image analysis. *Additive Manufacturing* **17**, 23–38 (2017)
- [9] Fu, Y., Downey, A.R., Yuan, L., Zhang, T., Pratt, A., Balogun, Y.: Machine learning algorithms for defect detection in metal laser-based additive manufacturing: A review. *Journal of Manufacturing Processes* **75**, 693–710 (2022)
- [10] Al-Maharma, A.Y., Patil, S.P., Markert, B.: Effects of porosity on the mechanical properties of additively manufactured components: a critical review. *Materials Research Express* **7**(12), 122001 (2020)
- [11] Yu, H., Yang, Z., Tan, L., Wang, Y., Sun, W., Sun, M., Tang, Y.: Methods and datasets on semantic segmentation: A review. *Neurocomputing* **304**, 82–103 (2018)
- [12] Nalajam, P.K., Ramesh, V.: Microstructural porosity segmentation using machine learning techniques in wire-based direct energy deposition of aa6061. *Micron* **151**, 103161 (2021)
- [13] Khan, I.A., Birkhofer, H., Kunz, D., Lukas, D., Ploshikhin, V.: A random forest classifier for anomaly detection in laser-powder bed fusion using optical monitoring. *Materials* **16**(19), 6470 (2023)
- [14] Bernsen, J.: Dynamic thresholding of grey-level images fcv. In: *Proceeding of the 8 International Conference O11 Pattern Rec-Gn Ition*, pp. 125–1255 (1986)

- [15] Otsu, N.: A threshold selection method from gray-level histograms. *IEEE Transactions on Systems, Man, and Cybernetics* **9**(1), 62–66 (1979) <https://doi.org/10.1109/TSMC.1979.4310076>
- [16] Ronneberger, O., Fischer, P., Brox, T.: U-net: Convolutional networks for biomedical image segmentation. In: *Medical Image Computing and Computer-Assisted Intervention—MICCAI 2015: 18th International Conference, Munich, Germany, October 5–9, 2015, Proceedings, Part III* 18, pp. 234–241 (2015). Springer
- [17] Scime, L., Siddel, D., Baird, S., Paquit, V.: Layer-wise anomaly detection and classification for powder bed additive manufacturing processes: A machine-agnostic algorithm for real-time pixel-wise semantic segmentation. *Additive Manufacturing* **36**, 101453 (2020)
- [18] Wong, V.W.H., Ferguson, M., Law, K.H., Lee, Y.-T.T., Witherell, P.: Automatic volumetric segmentation of additive manufacturing defects with 3d u-net. *arXiv preprint arXiv:2101.08993* (2021)
- [19] Ziabari, A., Venkatakrisnan, S., Snow, Z., Lisovich, A., Sprayberry, M., Brackman, P., Frederick, C., Bhattad, P., Graham, S., Bingham, P., *et al.*: Enabling rapid x-ray ct characterisation for additive manufacturing using cad models and deep learning-based reconstruction. *npj Computational Materials* **9**(1), 91 (2023)
- [20] Van Opbroek, A., Ikram, M.A., Vernooij, M.W., De Bruijne, M.: Transfer learning improves supervised image segmentation across imaging protocols. *IEEE transactions on medical imaging* **34**(5), 1018–1030 (2014)
- [21] Ouidadi, H., Xu, B., Guo, S.: Defect segmentation from x-ray computed tomography of laser powder bed fusion parts: A comparative study among machine learning, deep learning, and statistical image thresholding methods. In: *International Manufacturing Science and Engineering Conference*, vol. 87233, pp. 001–01012 (2023). American Society of Mechanical Engineers
- [22] Bommasani, R., Hudson, D.A., Adeli, E., Altman, R., Arora, S., Arx, S., Bernstein, M.S., Bohg, J., Bosselut, A., Brunskill, E., *et al.*: On the opportunities and risks of foundation models. *arXiv preprint arXiv:2108.07258* (2021)
- [23] Kirillov, A., Mintun, E., Ravi, N., Mao, H., Rolland, C., Gustafson, L., Xiao, T., Whitehead, S., Berg, A.C., Lo, W.-Y., *et al.*: Segment anything. *arXiv preprint arXiv:2304.02643* (2023)
- [24] Jia, M., Tang, L., Chen, B.-C., Cardie, C., Belongie, S., Hariharan, B., Lim, S.-N.: Visual prompt tuning. In: *European Conference on Computer Vision*, pp. 709–727 (2022). Springer
- [25] Liu, P., Yuan, W., Fu, J., Jiang, Z., Hayashi, H., Neubig, G.: Pre-train, prompt, and predict: A systematic survey of prompting methods in natural language

- processing. *ACM Computing Surveys* **55**(9), 1–35 (2023)
- [26] Lin, Z., Zhang, Z., Chen, L.-Z., Cheng, M.-M., Lu, S.-P.: Interactive image segmentation with first click attention. In: *Proceedings of the IEEE/CVF Conference on Computer Vision and Pattern Recognition*, pp. 13339–13348 (2020)
- [27] Brown, T., Mann, B., Ryder, N., Subbiah, M., Kaplan, J.D., Dhariwal, P., Neelakantan, A., Shyam, P., Sastry, G., Askell, A., *et al.*: Language models are few-shot learners. *Advances in neural information processing systems* **33**, 1877–1901 (2020)
- [28] Haas, L., Alberti, S., Skreta, M.: Learning generalized zero-shot learners for open-domain image geolocalization. *arXiv preprint arXiv:2302.00275* (2023)
- [29] Ramesh, A., Pavlov, M., Goh, G., Gray, S., Voss, C., Radford, A., Chen, M., Sutskever, I.: Zero-shot text-to-image generation. In: *International Conference on Machine Learning*, pp. 8821–8831 (2021). PMLR
- [30] Ma, J., Wang, B.: Towards foundation models of biological image segmentation. *Nature Methods* **20**(7), 953–955 (2023)
- [31] Vaswani, A., Shazeer, N., Parmar, N., Uszkoreit, J., Jones, L., Gomez, A.N., Kaiser, L., Polosukhin, I.: Attention is all you need. *Advances in neural information processing systems* **30** (2017)
- [32] Alzubaidi, L., Zhang, J., Humaidi, A.J., Al-Dujaili, A., Duan, Y., Al-Shamma, O., Santamaría, J., Fadhel, M.A., Al-Amidie, M., Farhan, L.: Review of deep learning: Concepts, cnn architectures, challenges, applications, future directions. *Journal of big Data* **8**, 1–74 (2021)
- [33] Singla, V., Ge, S., Ronen, B., Jacobs, D.: Shift invariance can reduce adversarial robustness. *Advances in Neural Information Processing Systems* **34**, 1858–1871 (2021)
- [34] Dosovitskiy, A., Beyer, L., Kolesnikov, A., Weissenborn, D., Zhai, X., Unterthiner, T., Dehghani, M., Minderer, M., Heigold, G., Gelly, S., *et al.*: An image is worth 16x16 words: Transformers for image recognition at scale. *arXiv preprint arXiv:2010.11929* (2020)
- [35] Maurício, J., Domingues, I., Bernardino, J.: Comparing vision transformers and convolutional neural networks for image classification: A literature review. *Applied Sciences* **13**(9), 5521 (2023)
- [36] Chen, A., Yao, Y., Chen, P.-Y., Zhang, Y., Liu, S.: Understanding and improving visual prompting: A label-mapping perspective. In: *Proceedings of the IEEE/CVF Conference on Computer Vision and Pattern Recognition*, pp. 19133–19143 (2023)

- [37] Zhou, Z.-H.: A brief introduction to weakly supervised learning. *National science review* **5**(1), 44–53 (2018)
- [38] OpenCV Thresholding Tutorial. https://docs.opencv.org/3.4/d7/d4d/tutorial_py_thresholding.html. Accessed: `{access date}`
- [39] Huang, T., Yang, G., Tang, G.: A fast two-dimensional median filtering algorithm. *IEEE Transactions on Acoustics, Speech, and Signal Processing* **27**(1), 13–18 (1979) <https://doi.org/10.1109/TASSP.1979.1163188>
- [40] Carass, A., Roy, S., Gherman, A., Reinhold, J.C., Jesson, A., Arbel, T., Maier, O., Handels, H., Ghafoorian, M., Platel, B., *et al.*: Evaluating white matter lesion segmentations with refined sørensen-dice analysis. *Scientific reports* **10**(1), 8242 (2020)
- [41] Guo, J., Yu, X., Wang, L.: Unsupervised anomaly detection and segmentation on dirty datasets. *Future Internet* **14**(3), 86 (2022)
- [42] Yi, J., Yoon, S.: Patch svdd: Patch-level svdd for anomaly detection and segmentation. In: *Proceedings of the Asian Conference on Computer Vision* (2020)
- [43] Thompson, A., Maskery, I., Leach, R.K.: X-ray computed tomography for additive manufacturing: a review. *Measurement Science and Technology* **27**(7), 072001 (2016)
- [44] Zhang, J., Zhao, X., Yang, B., Li, J., Liu, Y., Ma, G., Yuan, S., Wu, J.: Non-destructive evaluation of porosity in additive manufacturing by laser ultrasonic surface wave. *Measurement* **193**, 110944 (2022)
- [45] Kumar, S., Tiwari, P., Zymbler, M.: Internet of things is a revolutionary approach for future technology enhancement: a review. *Journal of Big data* **6**(1), 1–21 (2019)
- [46] He, K., Chen, X., Xie, S., Li, Y., Dollár, P., Girshick, R.: *Masked Autoencoders Are Scalable Vision Learners* (2021)
- [47] Bahng, H., Jahanian, A., Sankaranarayanan, S., Isola, P.: Exploring visual prompts for adapting large-scale models. *arXiv preprint arXiv:2203.17274* (2022)